Non-Contact Pulmonary Functional Testing through an improved Photometric Stereo Approach

Jahanzeb Ahmad
jahanzeb.ahmad@uwe.ac.uk

Jiuai Sun
jiuai2.sun@uwe.ac.uk

Lyndon Smith
lyndon.smith@uwe.ac.uk

Melvyn Smith
melvyn.smith@uwe.ac.uk

Center of Machine Vision,
Bristol Robotics Laboratory,
University of the West of England,
Bristol, UK

Abstract

A non-contact computer vision based system is developed for Pulmonary Functional Testing. The unique and novel features of the system are that it views the patients from both front and back and creates a 3D structure of the whole torso. By observing the 3D structure of the torso over time, the amount of air inhaled and exhaled is estimated. The Photometric Stereo method is used to recover local 3D surface orientation. This technique is good for recovering the local 3D surface orientation but provides no absolute depth information about the observed scene. To calculate absolute depth information from Photometric Stereo a new Lambertian Diffused Maxima Region (DMR) based algorithm is employed here. A high (0.96) correlation between breathing volume calculated from Photometric Stereo and Spirometer data is observed.

1 Introduction

The most common test performed on patients to assess their respiratory functionality is known as the Pulmonary Functionality Test (PFT). This test measures the flow and volume of air inspired and expired from lungs using device called a Spirometer. The contact based nature of the devices increases breath awareness which may cause hyperventilation and alter the breathing pattern [5, 6]. In addition, a high degree of compliance is required from patient which is not always possible because of the contact based nature of Spirometer. Recent advancements in computer vision and computing have enabled researchers to develop non-invasive non-contact systems to overcome the problem due to the contact based nature of Spirometers .

The pioneering work in development of a vision based Spirometer was done by Ferrigno and Pedotti [4] in 1985 and their system was called The "ELITE" (ELITE System; BTS, Milan, Italy). Ferrigno and Pedotti placed predefined markers on the patient's torso and used a digital video motion analyser system to track markers. Aoki et al [1] in 2005 presented a
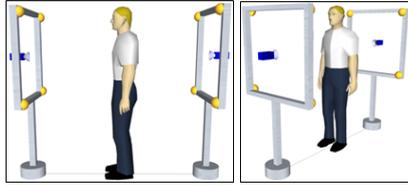
Figure 1: Photometric stereo Rig with subject standing in middle of two rigs.

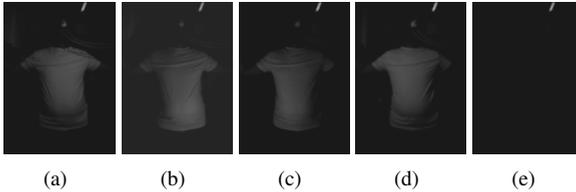|				
(a)	(b)	(c)	(d)	(e)

Figure 2: Raw Images obtained from FrontRig. Image(a) when top-right light is turned on, image(b) when bottom-right light is turned on, image(c) when bottom-left light is turned on, image(d) when top-left light is turned on and image(e) when no light is turned on.

triangulation based respiration monitoring and measurement method. The system was based on a fibre grating vision sensor, which is composed of a multiple slit light projector and a CCD camera. Recently a group of researchers from Cambridge University, Cambridge UK and PneumaCare Limited, Duxford UK have developed a new Non-Contact (marker-less) system called Structured Light Plethysmography(SLP) for respiratory functional testing [2].

In this paper we present a novel Photometric Stereo [7] based method for performing pulmonary functional testing through surface gradient analysis. Photometric stereo (PS) is able to recover the surface shape of an object or scene by means of several images taken from a same view point but under different lighting conditions. At least three images are needed to estimate the surface gradient using Photometric Stereo. In our setup we use five images to estimate surface gradient; four images are taken by turning on one light source at a time as shown in Figure 2(a) to Figure 2(d). Light sources are placed at equal distance from each other to get homogenous light distribution among all four images as shown in Figure 1. The fifth image is taken when no light source is turned on to get the background light intensity (noise) as shown in Figure 2(e). As the images are taken in an unconstrained office room environment, there is a fluorescent tube light on ceiling is clearly visible in Figure 2.

2   Surface gradient and volume estimation

According to the Lambertian reflectance model the intensity I of light reflected from an object's surface is dependent on the surface albedo ρ and the cosine of the angle of the incident light as described in Equation 1. The cosine of the incident angle can also be referred as dot product of the unit vector of the surface normal N and the unit vector of light source direction $\vec{L}$, as shown in Equation 2. When more than two images from same view point are available under different light conditions, we have a linear set of equations 1 and 2 and this

can be represented in vector form as shown in equation 3.

$$I = cos(\phi_i) \tag{1}$$

$$I = (L \cdot N) \tag{2}$$

$$\vec{I}(x,y) = (x,y)[L]\vec{N}(x,y) \tag{3}$$

In our case $\vec{I}$ is the vector formed by the four pixels $((I^1(x,y), I^2(x,y), I^3(x,y), I^4(x,y))$ from four images, [L] is the matrix composed by the light vectors $(\vec{L^1}, \vec{L^2}, \vec{L^3}, \vec{L^4})$. 1, 2, 3 and 4 is the number with respect to the individual light source direction and (x,y) is pixel position in spatial domain. These light directions are calculated during a calibration process using a specular sphere. [L] is not a square and so not invertible, but the local surface gradients p(x,y) and q(x,y), and the local surface normal N(x,y) can be calculated from the least square method using equations 4 and 5.

$$\vec{M}(x,y) = ([L]^T[L])^{-1}[L]^T\vec{I}(x,y) = (m_1(x,y), m_2(x,y), m_3(x,y)) \tag{4}$$

$$p(x,y) = \frac{-m_1(x,y)}{m_3(x,y)}, q(x,y) = \frac{-m_2(x,y)}{m_3(x,y)} \tag{5}$$

The volume of the torso is represented as the total average gradient; we call it the gradient volume (GV). GV is calculated by adding the absolute average of p and q and then normalizing it as shown in equation 6 and equation 7 for both front and back. Where k and l are the total number of valid pixels in the front and back images respectively, p_f, q_f are the local surface gradients of front image and p_b, q_b are the local surface gradients of the back image. To compare GV with volume obtained from a Pneumotachometer, normalization is applied on both signals using equation 7. $\bar{V}$ represents mean value of V.

$$V = [\frac{1}{k}\sum(|p_f| + |q_f|)] + [\frac{1}{l}\sum(|p_b| + |q_b|)] \tag{6}$$

$$GV = \frac{(V - \bar{V}}{max(|V - \bar{V}|)} \tag{7}$$

3 Object distance estimation

The object distance from the camera is estimated by using the Diffused Maxima Region (DMR), which is calculated by taking an absolute of dot product between the pseudo light vector and pseudo surface normal and then applying a threshold (th) as shown in equation 8.

$$DMR_i = |N \cdot S^i| > th \tag{8}$$

S^i is a pseudo light vector for light i and N is the pseudo surface normal at each pixel. Pseudo light vector (S^i) is calculated during the calibration process by placing the sphere at the centre of the field of view, it is assumed to be the same for every pixel. The estimated centre of the DMR gives us the point where the surface normal and the light vector are approximately aligned. Many DMR(s) can exist on the surface of an object but the region with
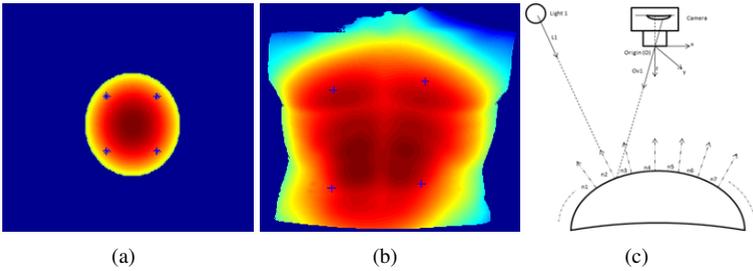
Figure 3: Diffused Maxima Regions centres of synthetic sphere (a) and real human dummy (b). Depth Calculation using DMR and intersection of vector Ov1 and L1 (c).
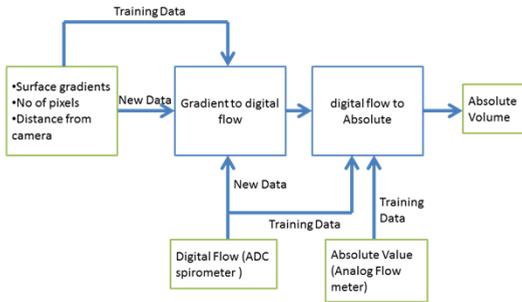

Figure 4: Gradient Volume to Absolute volume conversion.

maximum area is considered to be the best choice. DMR can also be selected on the basis of shape or location but experiments have shown that using maximum area as a selection criterion produces best results. Figure 3(a-b) shows the four selected DMR centres on a height map of a synthetic sphere and a real human dummy.

Once the DMR centre is identified in the image plane a vector Ov1 can be created from the DMR centre to the centre of the lens (O) as shown in Figure 3(c). Now by using origin (O), position of light (LP), light vector L1 and vector Ov1 we can determine the intersection point of these two vectors in world coordinates [3]. That effectively gives the knowledge of the scene range from the camera and light sources.

4   Calculating absolute amount of air volume

The air volume calculated from photometric stereo in section 2 does not give the absolute amount of air. To calculate absolute amount of air from surface gradient we use two calibration steps. The first calibration step is to convert the gradient information into digital flow value which is achieved through linear regression and this digital flow value is converted to absolute air volume in a second step by using linear curve fitting. The flow of data and calibration process is shown in Figure 4.

The least square method is used for regression, given surface gradient calculated using Photometric Stereo, number of pixels obtained from segmentation and distance of object from camera calculated using diffused maxima, a feature matrix [X] ($X = [gradient\ pixels\ distance]$) is constructed. The signal obtained from a Pneumotachometer is digitized using analog to
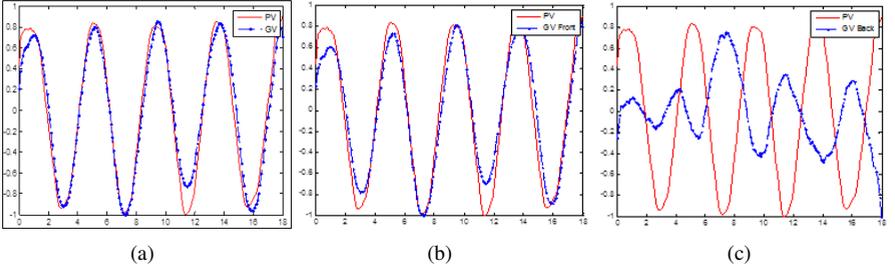
| (a) | (b) | (c) |

Figure 5: Figure a:Comparison of Pneumotachometer Volume (PV) and Gradient Volume (GV) (combined front and back). Figure b: front Gradient Volume (GV) and Pneumotachometer Volume (PV) plot, Figure c: back GV and PV plot. Horizontal axis is time in seconds. Vertical scale is a normalized representation of volume.

digital converter (ADC) and is represented as pv. ϕ ($\phi = (X' * X)^{-1} * X' * pv$) is trained using [X] and pv ($pv_2 = X_2 * \phi$). Where $[X_2]$ is new input and pv_2 is the synthesised digital Pneumotachometer signal which will be converted to absolute air volume using curve fitting.

The absolute amount of air inhaled and exhaled is calculated from digital flow by using linear curve fitting. The coefficients of the curve fitting equation are calculated using values obtained from a carefully controlled air flow meter, by digitizing the flow using an analogue to digital converter and transducer. Absolute amount of air is calculated by $absolute volume = C_1 * pv_2 + C_0$. Where $C_1 = 0.002085, C_0 = -4.007$

5 Results

High correlation (0.98) between gradient volume and Pneumotachometer volume (Ground Truth) was found as shown in Figure 5(a). It also reflects the effect of error in surface gradient is very minimal on volume calculation because of the normalization and calibration processes used to calculate the relative and absolute amount of air.

Analysis on the front and back has been performed independently, which suggests that the correlation of the back gradient volume is negatively correlated to the Pneumotachometer volume and front gradient volume is positively correlated to Pneumotachometer volume. Front GV shows high correlation with PV but when back GV, which is weakly and negatively correlated with PV, is added to front GV it yields higher correlation as compared to front GV only. This phenomenon is shown in Figure 5(b-c).

After the calibration process of converting the relative GV to absolute air volume the correlation drops from 0.98 to 0.96. This is due to errors introduced during the training and curve fitting process involved in calibration steps. The experiments have been performed on 6 healthy subjects and results have been summarised in Table 1. Table 1 shows high degree of correlation between air volume obtained from Pneumotachometer and air volume estimated from photometric stereo images.

6 Conclusion and future work

We have proposed a novel non-contact approach and designed a device to perform Pulmonary Functional Testing (PFT) on patients of any age. The unique features of the device

Table 1: Correlation between PV and Absolute GV.

	Correlation between PV and Absolute GV
Subject 1	0.960
Subject 2	0.935
Subject 3	0.963
Subject 4	0.958
Subject 5	0.916
Subject 6	0.922

are that it needs very little calibration and no registration between front and back view, and generates at least 2000 times higher resolution data compared to similar systems. We also presented a method to calculate the distance of object from a camera using photometric stereo images which gives the absolute amount of air inhaled and exhaled. As the system is based on off the shelf low-cost components it is relatively easy and cheap to make. In future we are planning to use the device for detecting a range of chest and back bone problems and take advantage of the high resolution 3D recovery for regional analysis of the torso.

References

[1] H. Aoki, K. Koshiji, H. Nakamura, Y. Takemura, and M. Nakajima. Study on respiration monitoring method using near-infrared multiple slit-lights projection. *IEEE International Symposium on Micro-NanoMechatronics and Human Science*, pages 291–296, 2005. doi: 10.1109/MHS.2005.1590006.

[2] Willem de Boer, Joan Lasenby, Jonathan Cameron, Rich Wareham, Shiraz Ahmad, Charlotte Roach, Ward Hills, and Richard Iles. SLP: A Zero-Contact Non-Invasive Method for Pulmonary Function Testing. *British Machine Vision Conference 2010*, pages 85.1–85.12, 2010. doi: 10.5244/C.24.85.

[3] F Dunn and I Parberry. *3D math primer for graphics and game development*. Wordware Publishing, Inc, 2011. ISBN 1556229119.

[4] Giancarlo Ferrigno and Antonio Pedotti. ELITE: a digital dedicated hardware system for movement analysis via real-time TV signal processing. *Biomedical Engineering, IEEE . . .*, BME-32(11):943–950, 1985.

[5] R. Gilbert and JH Auchincloss. Changes in tidal volume, frequency, and ventilation induced by their measurement. *Journal of Applied . . .*, 33(2):252–254, 1972.

[6] E Schneider, C Dualé, J-L Vaille, L Ouchchane, T Gillart, D Guélon, and P Schoeffler. Comparison of tolerance of facemask vs. mouthpiece for non-invasive ventilation. *Anaesthesia*, 61(1):20–3, January 2006. ISSN 0003-2409. doi: 10.1111/j.1365-2044.2005.04400.x.

[7] RJ Woodham. Photometric method for determining surface orientation from multiple images. *Optical engineering*, 19(1):139–144, 1980.